Biosensors and Bioelectronics 31 (2012) 544–547

Contents lists available at SciVerse ScienceDirect

Biosensors and Bioelectronics

journal homepage: www.elsevier.com/locate/bios

Short communication

A novel enzymatic hydrogen peroxide biosensor based on Ag/C nanocables

Chang-Jie Mao[a], Xi-Bao Chen[a], He-Lin Niu[a,*], Ji-Ming Song[a], Sheng-Yi Zhang[a], Rong-Jing Cui[b,*]

[a] School of Chemistry and Chemical Engineering, Anhui University, Hefei 230039, China
[b] Jiangsu Laboratory of Advanced Functional Materials, Department of Chemistry and Materials Engineering, Changshu Institute of Technology, Changshu 215500, China

ARTICLE INFO

Article history:
Received 13 July 2011
Received in revised form 1 October 2011
Accepted 3 October 2011
Available online 12 October 2011

Keywords:
Ag/C nanocables
Biosensor
Horseradish peroxidase
Hydrogen peroxide

ABSTRACT

A novel enzymatic hydrogen peroxide sensor was successfully fabricated based on the nanocomposites containing of Ag/C nanocables and gold nanoparticles (AuNPs). Ag/C nanocables have been synthesized by a hydrothermal method and then AuNPs were assembled on the surface of Ag/C nanocables. The nanocomposites were confirmed by X-ray diffraction (XRD), transmission electron microscopy (TEM), scanning electron microscopy (SEM) and energy-dispersive X-ray spectrometry (EDS). The above nanocomposites have satisfactory chemical stability and excellent biocompatibility. Cyclic voltammetry (CV) was used to evaluate the electrochemical performance of the Ag/C/Au nanocomposites at glassy carbon electrode (GCE). The results indicated that the Ag/C/Au nanocomposites exhibited excellent electrocatalytic activity to the reduction of H_2O_2. It offered a linear range of 6.7×10^{-9} to 8.0×10^{-6} M, with a detection limit of 2.2×10^{-9} M. The apparent Michaelis–Menten constant of the biosensor was 51.7×10^{-6} M. These results indicated that Ag/C/Au nanocomposites have potential for constructing of a variety of electrochemical biosensors.

1. Introduction

Attentions have been focused on accurate detection of hydrogen peroxide (H_2O_2), due to their important role in food, pharmaceutical, industrial and environmental monitoring (Jia et al., 2009). Many techniques including spectrometry (Matsubara et al., 1992), fluorescence (Li and Dasgupta, 2000), chemiluminescence (Kricka et al., 1996), and electrochemistry (Xu et al., 2007), have been employed for the determination of H_2O_2. Among these methods, enzyme-based electrochemical biosensors with the intrinsic selectivity and sensitivity of enzymatic reactions have been considered as the most effective measure. Particularly, the third generation biosensor based on the direct electron transfer between an electrode and immobilized peroxidase has been extensively explored in the determination of H_2O_2 during the past decade (Wong and Schwaneberg, 2003). These third-generation biosensors can permit the sensitive and convenient electrochemical measurement of the enzyme substrate without the addition of a mediator (Willner and Katz, 2000). However, it is generally difficult to achieve direct electron transfer between enzymes and the electrodes due to the deeply embedded redox-active center, unfavorable orientation and denature of enzymes (Xu et al., 2006). To overcome these shortcomings, nanomaterials as immobilization material have been successfully used in the fabrication of enzymes modified electrodes. For example, Dong group fabricated HRP/Au NPs/sol–gel network on a gold electrode using the direct coupling of sol–gel and self-assembled technologies. Since Au NPs allow efficient electron tunneling and can assist the electron transfer, the as-modified electrode displayed a significant amplification of the electrochemical response to H_2O_2 detection (Jia et al., 2002).

Metal nanomaterials have attracted specific interest for widely applied in various fields. Among all metals, silver (Ag) nanomaterials have exhibited the highest thermal and electrical conductivity and widely used in electronics, photonics, biological labeling, and surface-enhanced Raman scattering (Song et al., 2008; De et al., 2009; Sun, 2010). However, they were very sensitive to air and moisture and easy aggregation. Therefore, one of the main problems in the application of Ag nanomaterials was the surface modification with various materials, which can make them to achieve desirable surface functionalities (Katz et al., 2005). Carbon (C) has been found to be attractive for functionalizing materials for excellent binding capability, conductivity, biocompatibility and solubility. Thus, the solubility and stability can be greatly improved by combining Ag with C. For example, Zhang et al. (2010) fabricated a biocompatible and conductive platform based on DNA/graphene nanocomposite for direct electrochemistry.

Gold nanoparticles (AuNPs) have also attracted much more attention for that they can strongly adsorb some proteins and effectively retain their biological activity (Brown et al., 1996). In most of the cases, the AuNPs provided a congenial microenvironment for the immobilization of proteins (Willner et al., 1994; Dequarie et al.,

* Corresponding authors. Tel.: +86 551 3861279.
E-mail addresses: niuhelin@gmail.com (H.-L. Niu), rongjingcui@gmail.com (R.-J. Cui).

0956-5663/$ – see front matter © 2011 Elsevier B.V. All rights reserved.
doi:10.1016/j.bios.2011.10.001

2000; Chen et al., 2006), and allowed the protein molecule more freedom in orientation, thus facilitated close approach of the protein to the sensing surface, reduced the insulating property of the protein shell for the direct electron transfer between the electrode and the immobilized HRP on the biosensor. On the other hand, the electrical conductivity of conducting materials, such as graphene and polyaniline, can be greatly increased if it was combined with Au NPs (Liu et al., 2008, 2010). However, few studies on the combination of Au NPs with Ag/C nanocables have been carried out, especially the application in biosensors.

Here, Ag/C nanocables were firstly synthesized, and then coated by Au nanoparticles. Combining with the advantages of Ag/C nanocables and Au NPs, the nanocomposites have many excellent properties, such as good solubility, biocompatibility, and high electrical conductivity (Cui et al., 2008). In addition, the nanocomposites were in favor of enhancing protein loading and retaining the bioactivity. Using horseradish peroxidase (HRP) as a model protein, the constructed biosensor displayed a fast electron transfer of HRP and an excellent electrochemistry activity for the detection of H_2O_2 with wide linear range and low detection limit. Therefore, the present work offers a new avenue to broaden the applications of Ag/C nanocables in electrochemical biosensors.

2. Experimental

2.1. Chemicals

HRP (EC 1.11.1.7, 250 U mg^{-1}) was purchased from Sigma and used as received. 0.1 M PBS of various pHs were prepared by mixing the stock solutions of NaH_2PO_4 and Na_2HPO_4, and then adjusting the pH with 0.1 M NaOH and H_3PO_4. Poly(diallyldimethylammonium chloride) (PDDA, 20%, w/w in water, MW = 200,000–350,000) were purchased from Sigma–Aldrich. All chemicals and solvents were analytical grade and all solutions were made up with twice-distilled deionized water.

2.2. Synthesis of Ag/C/Au nanocomposites

Ag/C nanocables were prepared according to the literature (Niu et al., in press). In a typical process, 0.015 mol of glycerol was dissolved in 30 mL of 0.5 mol/L H_2SO_4 solution and then 0.0015 mol of $AgNO_3$ was added into the above solution. This solution mixture was then placed into a 50 mL teflon-lined stainless steel autoclave, sealed and maintained at 180 °C for 12 h. On cooling the sample at room temperature, the precipitate was separated by centrifuging at a rotation rate of 9000 rpm for 10 min. It was then washed with distilled water and absolute ethanol in sequence, and dried in air at room temperature. The Au colloid was prepared by reducing $HAuC1_4$ aqueous solution with trisodium citrate according to the literature (Enustun and Turkevich, 1963). The average diameter of the prepared Au NPs is about 20 nm.

The mixture solution containing 10 mL 0.2% PDDA and 0.5 mol/L NaCl was added into 20 mg Ag/C nanocable, sonicated for 10 min, centrifuged and washed. Then 15 mL Au colloid added into the above solution. After continuing vigorously stirring the solution for 10 h, the deposit was collected, washed with deionized water several times. Finally, the as-prepared nanocomposites with the concentration of 5 mg/mL were obtained.

2.3. Preparation of Ag/C/Au/HRP nanocomposites modified glassy carbon (GCE) electrode

The GCE with a diameter of 3 mm was used as the substrate to grow the Ag/C/Au/HRP nanocomposites film. Prior to preparation procedure of the films, the GCE was successively polished to a mirror finish using 0.3 and 0.05 μm alumina slurry (Beuhler) followed by rinsing thoroughly with water. After successive sonication in 1:1 nitric acid, acetone, and doubly distilled water, the electrode was rinsed with doubly distilled water and allowed to dry at room temperature.

The HRP stock solution was prepared by dissolving 5 mg HRP in 1 mL phosphate buffer solution (PBS, pH 7.0). Then, 100 μL of the HRP solution was mixed with 100 μL of the Ag/C/Au nanocomposites. The resultant colloidal solution (3 μL) was then dropped onto the pretreated electrode surface and allowed to dry under ambient conditions. Then 0.1% Nafion (3 μL) was subsequently dropped onto the Ag/C/Au nanocomposites-modified GCE and dried under ambient conditions.

2.4. Apparatus

Powder X-ray diffraction (XRD) was conducted on a MAP18XAHF X-ray diffractometer (MAC Science Ltd., Japan). TEM images were recorded on a JEM-2100 transmission electron microscope (JEOL Ltd., Japan). SEM images were taken by an S-4800 scanning electron microscope (Hitachi Ltd., Japan). EDS analysis was carried out by using a SEM equipped with an energy-dispersive X-ray detector.

Cyclic voltammetric and amperometric experiments were conducted with a CHI660D workstation (Shanghai Chenhua, China). All experiments were carried out using a conventional three-electrode system in 0.2 M phosphate buffer solution (PBS), where nanocomposite-modified GCE was used as the working electrode, a platinum wire as the auxiliary electrode and a saturated calomel electrode (SCE) as the reference electrode.

3. Results and discussion

3.1. Characterization

XRD was carried out to characterize the as-prepared products. The X-ray diffraction (XRD) pattern of the obtained Ag/C nanocables was shown in Fig. 1A. All diffraction peaks could be perfectly indexed to the face-centered silver (JCPDS card No. 4-0783). It can be observed in Fig. 1B that carbon has covered the surface of Ag nanowires and the obtained Ag/C nanocables were uniform in size and morphology with an average diameter of 50 nm and smooth surface. Fig. 1C and D shows the typical TEM and SEM images of the Ag/C/Au nanocomposite. It can be clearly seen that the Au NPs are uniformly adsorbed onto the Ag/C nanocables. The as-prepared nanocomposites were also characterized by EDS, indicating that Au NPs indeed existed in the nanocomposites (inset Fig. 1D).

3.2. Electrochemistry of the biosensor

Fig. 2A showed the CVs of (a) bare GCE, (b) Ag/C/Au/GCE, (c) Ag/C/HRP/GCE, and (d) Ag/C/Au/HRP/GCE in pH 7.0 PBS at 100 mV/s, respectively. No obvious redox peaks were observed at the bare GCE (curve a) and Ag/C/Au/GCE (curve b), which suggests that neither Ag/C nanocable nor Ag/C/Au nanocomposites were electroactive in the potential range studied. The CV of Ag/C/HRP/GCE (curve c) had a pair of quasi-reversible redox peaks, implying direct electron transfer between the immobilized HRP and the electrode. In comparison, the redox peaks observed on the Ag/C/Au/HRP/GCE (curve d) were remarkably large. The cathodic and anodic peak potentials were −0.437 V and −0.405 V, respectively. The formal potential (E_p), calculated from the average value of cathodic and anodic peak potentials, was −0.421 V, which is characteristic of the reversible electrode process of the heme Fe(III)/Fe(II) redox couple in immobilized HRP. This result demonstrated that the Ag/C

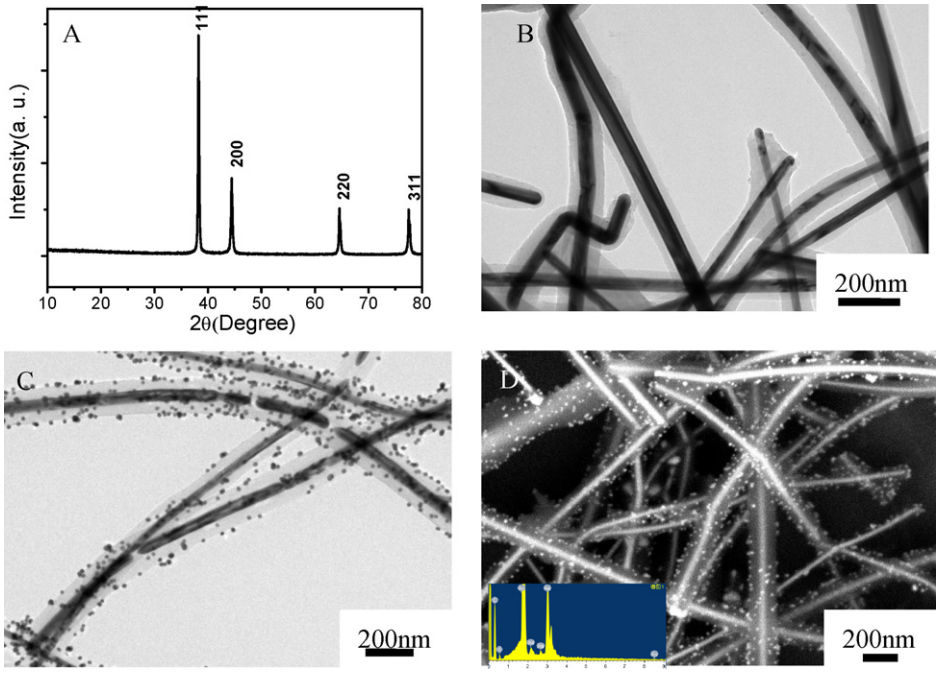

Fig. 1. (A) XRD pattern and (B) TEM of Ag/C nanocables. (C) TEM and (D) SEM of Ag/C/Au nanocomposites (inset: EDS data).

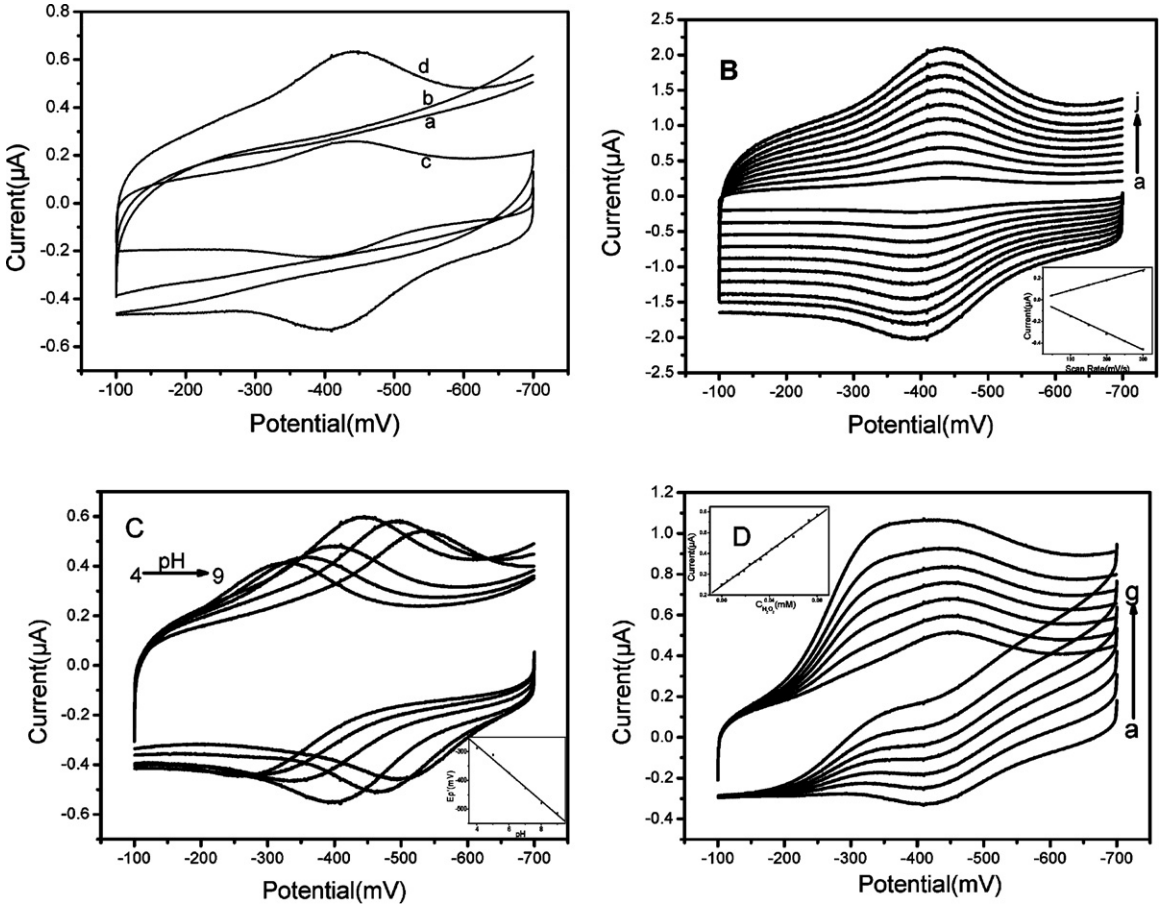

Fig. 2. (A) CVs obtained at (a) bare GCE, (b) Ag/C/Au/GCE, (c) Ag/C/HRP/GCE, and (d) Ag/C/Au/HRP/GCE in PBS 7.0 at 100 mV/s. (B) CVs of Ag/C/Au/HRP/GCE measured in the PBS 7.0 (0.2 M) at the different scan rates (a: 50 mV/s, b: 100 mV/s, c: 150 mV/s, d: 200 mV/s, e: 250 mV/s, f: 300 mV/s, g: 350 mV/s, h: 400 mV/s, i: 450 mV/s and j: 500 mV/s). Inset (B) calibration plot of the peak current and the scan rate. (C) CVs of Ag/C/Au/HRP/GCE measured in 0.2 M PBS with different pH value. Inset (C) calibration plot of peak potential and pH value respectively. (D) CVs of Ag/C/Au/HRP/GCE in the present of H_2O_2 with different concentration (a: 0 M, b: 6.67×10^{-9} M, c: 1.4×10^{-6} M, d: 2.33×10^{-6} M, e: 3.73×10^{-6} M, f: 5.33×10^{-6} M, g: 8.004×10^{-6} M). Inset (D) calibration plot of response current and H_2O_2 concentration.

nanocable played an important role in facilitating direct electron transfer between HRP and the GC electrode. Being a nanocomposite, Ag/C/Au combined the advantages of both components, such as the good biocompatibility of Ag/C nanocable and the excellent electron-transport properties and large surface area of AuNPs, which could provide a conductive and favorable microenvironment for the immobilized HRP to realize direct electrochemistry.

The effect of scan rate (v) on the peak currents of the Ag/C/Au/HRP/GCE in the range from 50 to 500 mV/s was shown in Fig. 2B. With the increased of scan rate, the anodic peak potential shifted toward a more positive value and the cathodic peak potential shifted toward a more negative value. At the same time, ΔE_p was increased, and $E^{\rho'}$ kept constant. The peak currents increased linearly with the scan rate ranging from 50 to 500 mV/s (shown in curve b), which indicated that the electrode reaction was a typical of surface-controlled quasi-reversible process.

The pH value has strong effect on the voltammetry behavior of Ag/C/Au/HRP/GCE. As shown in Fig. 2C, both reduction and oxidation peaks shifted with increasing of pH between pH 4.0 and 9.0. The formal potential ($E^{\rho'} = (E_{pc} + E_{pa})/2$) shifted linearly to direction with increasing pH. The linear regression equations was $E^{\rho'} = -86.59 - 48.11$ pH ($R = 0.9999$), which indicated that pH has effect on redox process of protein.

Fig. 2D shows the CVs of Ag/C/Au/HRP/GCE in the present of H_2O_2 with different concentration. As shown in curve a, Ag/C/Au/HRP/GCE has a sensitive, fast and stability response of the addition of H_2O_2. This may be due to the improvement of the microenvironment for the electron transfer of HRP. Ag nanowire could also play a role of an efficient electron conducting tunnel and reduce the insulating of the protein shell for direct electron transfer. Furthermore, the strong adsorption of nanomaterials to HRP may reduce the denaturation of HRP on GCE and cause adsorbed protein to possess a favorable orientation for the direct electron transfer between HRP and GC electrode. Calibration plot of response current and H_2O_2 concentration was shown in curve b. The reduction peak currents were linearly proportional to H_2O_2 concentration (inset Fig. 2D) in the range from 6.7×10^{-9} to 8.0×10^{-6} M with a correlation coefficient of 0.9982. The detection limit was estimated to be 2.2×10^{-9} M, which was lower than the previously reported HRP-based modified electrode (Lu et al., 2006; Zhang et al., 2010). The high sensitivity suggested that the immobilized HRP on the Ag/C/Au nanocomposites matrix had good bioelectrocatalytic activity for H_2O_2. The apparent Michaelis–Menten constant of the H_2O_2 biosensor was 51.7 μM according to the Lineweaver–Burk equation.

3.3. Reproducibility and stability of the Ag/C/Au/HRP/GCE

The reproducibility was also detected with chronoamperometry test. The RSD is 4.6% for 7 successive measurements of 5 μM H_2O_2 in 0.1 M PBS (pH 7.0), which indicated that the modified electrode possessed good reproducibility. To investigate the stability of the Ag/C/Au/HRP/GCE, the modified electrode was stored in PBS at 4 °C and CVs were measured after a period of storage time. The decrease in the cathodic peak current was negligible after 24 h. For the chronoamperometry test, the response to 5 μM H_2O_2 retained 98% of its initial current after 24 h storage, which demonstrated that the Ag/C/Au/HRP/GCE was stable in buffer solution. The long-term stability of the Ag/C/Au/HRP/GCE was also tested. After the modified electrode had been stored at 4 °C for a week, the currents for the direct electron transfer of HRP and the responses to 5 μm H_2O_2 had not changed. Even after storage for a month, the reduction current of H_2O_2 still remained at 92% of its initial value. These results indicated that the Ag/C/Au/HRP/GCE had a good stability toward the electrocatalytic reduction of H_2O_2; this stability could be attributed to the good film forming ability and excellent biocompatibility of the Ag/C/Au nanocomposites.

4. Conclusion

In this paper, the Ag/C/Au nanocomposites modified glassy carbon electrode was applied to construct a H_2O_2 sensor. The above modified electrode showed high electrocatalytic activity to H_2O_2. With HRP as a model oxidase enzyme, we constructed a H_2O_2 biosensor through covalent immobilization of the enzyme on the Ag/C/Au nanocomposites. The developed H_2O_2 biosensor had high sensitivity, wide linear range, low detection limit and good reproducibility. Furthermore, Ag/C/Au nanocomposites could be a promising option for the development of various oxidase-based biosensors and bioelectronic devices.

Acknowledgements

This work was supported by the National Natural Science Foundation of China (Grant Nos. 20875001, 20905001, 20905010 and 21071002), Natural Science Foundation of Anhui Province (11040606Q02) and 211 project of Anhui University.

References

Brown, K.R., Fox, A.P., Natan, M.J., 1996. J. Am. Chem. Soc. 118, 1154–1157.
Chen, J., Tang, J.H., Yan, F., Ju, H.X., 2006. Biomaterials 27, 2313–2321.
Cui, R.J., Liu, C., Shen, J.M., Gao, D., Zhu, J.J., Chen, H.Y., 2008. Adv. Funct. Mater. 18, 2197–2204.
De, S., Higgins, T.M., Lyons, P.E., Doherty, E.M., Nirmalraj, P.N., Blau, W.J., Boland, J.J., Coleman, J.N., 2009. ACS Nano 3, 1767–1774.
Dequarie, M., Degr, C., Limoges, B., 2000. Anal. Chem. 72, 5521–5528.
Enustun, B.V., Turkevich, J., 1963. J. Am. Chem. Soc. 85, 3317–3328.
Jia, J.B., Wang, B.Q., Wu, A.G., Cheng, G.J., Li, Z., Dong, S.J., 2002. Anal. Chem. 74, 2217–2223.
Jia, N.Q., Lian, Q., Wang, Z.Y., Shen, H.B., 2009. Sens. Actuators B 137, 230–234.
Katz, E., Baron, R., Willner, I., 2005. J. Am. Chem. Soc. 127, 4060–4070.
Kricka, L.J., Ji, X., Thorpe, G.H.G., Edwards, B., Voyta, B., Bronstein, I., 1996. J. Immunoassay 17, 67–83.
Li, J., Dasgupta, P.K., 2000. Anal. Chem. 72, 5338–5347.
Liu, K.P., Zhang, J.J., Yang, G.H., Wang, C.M., Zhu, J.J., 2010. Electrochem. Commun. 12, 402–405.
Liu, Y.G., Feng, X.M., Shen, J.M., Zhu, J.J., Hou, W.H., 2008. J. Phys. Chem. B 112, 9237–9242.
Lu, X.B., Zhang, Q., Zhang, L., Li, J.H., 2006. Electrochem. Commun. 8, 874–878.
Matsubara, C., Kawamoto, N., Takamura, K., 1992. Analyst 117, 1781–1784.
Niu, H.L., Wu, X.H., Qiu, M., Gao, Y.H., Song, J.M., Mao, C.J., Zhang, S.Y., Liu, H.L., Wu, J.H., J. Mater. Res., doi:10.1557/jmr.2011.251, in press.
Song, X.C., Zhao, Y., Zheng, Y.F., Yang, E., Fu, J., He, Y., 2008. Cryst. Growth Des. 8, 1823–1826.
Sun, Y.G., 2010. J. Phys. Chem. C 114, 2127–2133.
Willner, I., Katz, E., 2000. Angew. Chem. Int. Ed. 39, 1180–1218.
Willner, I., Lapidot, N., Riklin, A., Kasher, R., Zahavy, E., Katz, E., 1994. J. Am. Chem. Soc. 116, 1428–1441.
Wong, T.S., Schwaneberg, U., 2003. Curr. Opin. Biotechnol. 14, 590–596.
Xu, Q., Mao, C., Liu, N.N., Zhu, J.J., Sheng, J., 2006. Biosens. Bioelectron. 22, 768–773.
Xu, S., Peng, B., Han, X., 2007. Biosens. Bioelectron. 22, 1807–1810.
Zhang, Q., Qiao, Y., Hao, F., Zhang, L., Wu, S.Y., Li, Y., Li, J.H., Song, X.M., 2010. Chem. Eur. J. 16, 8133–8139.